Poster3-21   **AN IMPROVED TECHNIQUE FOR ESTIMATING ZDR BIAS FROM LIGHT RAIN ON RADARS THAT DO NOT VERTICALLY POINT**

Lindsey M. Richardson* and Robert R. Lee
NEXRAD Radar Operations Center, Norman, Oklahoma, U.S.A.

1. INTRODUCTION

Differential Reflectivity is a dual-polarimetric variable with many factors able to impact its calibration. Hardware and software techniques have been explored in the radar community from built-in test signals to known-target estimation. Known-target estimation includes targets such as a tethered sphere (e.g., Atlas 2002; Bechini et al. 2010) or distributed weather targets such as light rain or snow crystals that have been compared with video disdrometers and particle imaging systems (e.g., Ryzhkov et al. 2005; Cao et al. 2008; Bechini et al. 2010). Vertical pointing is a type of known-target estimation assuming that the radar is scanning light rain/drizzle with little to no wind. Using information about the expected return in light rain can give an estimate of the total Differential Reflectivity (ZDR) Bias of the radar system (McCormick and Hendry 1975; Vivekanandan 2003). Due to a lack of appropriate weather and/or hardware constraints, some radar systems, such as the Weather Surveillance Radar – 1988 Dual-Polarimetric Doppler (WSR-88D), cannot use the Vertical Pointing Technique. Other known-target methods have been explored using information from non-vertical pointing radar returns of Light Rain, Dry Snow, and Bragg Scatter to estimate the ZDR Bias (Zittel et al. 2014; Zittel et al. 2015; Richardson et al. 2017 a,b). For each of the methods, the ZDR Bias is estimated as:

$$\text{ZDR Bias} = \text{ZDR}_{Measured} - \text{ZDR}_{Intrinsic} \qquad (1)$$

where $\text{ZDR}_{Measured}$ is the ZDR measured by the radar and $\text{ZDR}_{Intrinsic}$ is the expected ZDR value of a given target type.

The original Light Rain technique estimates ZDR Bias from light rain targets via known intrinsic values of ZDR related to certain levels of reflectivity (Z). Information from the Melting Layer Detection Algorithm (MLDA) ensure radar range gates used for estimating the bias are below the melting layer to avoid contamination from frozen particles or super-cooled liquid drops that have a different characteristic in ZDR (OFCM 2017). Reflectivity between 19.0 and 30.0 dBZ is considered below convective thresholds with some overlap with winter precipitation (Straka et al. 2000). Large drops and/or melting particles within this reflectivity range can impact the estimation of ZDR, ultimately resulting in a high bias in the estimate. Work by Schuur et al. (2001; 2005) has shown that the expected ZDR of rain between 19.0 and 30.0 dBZ

can range from 0.23 to 0.55 dB. Using an incorrect $\text{ZDR}_{Intrinsic}$ in this reflectivity range can introduce ZDR Bias estimation error and allow for larger variability of ZDR Bias Estimated from Light Rain (ZDRBELR).

Dry Snow estimates are taken from range gates above the melting layer and classified as Dry Snow based on the Hydrometeorological Classification Algorithm (HCA; Straka et al 2000; OFCM 2017). ZDR Bias Estimated from Dry Snow (ZDRBEDS) only uses radar range gates within the first 1 km height above the top of the estimated Melting Layer top. This particular region is known as a likely area to find dry aggregates instead of crystals (Meishner et al. 1991; Zittel et al. 2014; Williams et al. 2015a,b). Estimates can still be influenced by errors from the MLDA and/or the HCA such as capturing the incorrect top of the melting layer and receiving some partially melted particles with larger ZDR values. A single $\text{ZDR}_{Intrinsic}$ of 0.20 is used in the Dry Snow method. Using only one value reduces the chance for estimation variability but still includes potential error from not completely capturing the needed $\text{ZDR}_{Intrinsic}$ in a given distribution environment.

Instead of detecting a specific particle type, Bragg scatter comes from refractivity gradients related to clear air turbulence (e.g., Atlas 1959; Hardy and Katz 1969; Melnikov et al. 2011, 2013; Davison et al. 2013a,b). Being able to detect it depends upon on the transmitted wavelength – S-band radars, such as the WSR-88D, can detect it with adequate intensity while C-band and smaller wavelengths have more challenges detecting Bragg scatter (e.g., Knight and Miller 1998). Bragg scatter has an intrinsic ZDR value of ~0.0 dB, thus, it has the least risk of using an incorrect $\text{ZDR}_{Intrinsic}$ value when making the ZDR Bias estimate. Previous work has shown that estimates from Bragg scatter have the least variability compared to Light Rain or Dry Snow (e.g. Richardson et al. 2017b). The ZDR Bias Estimated from Bragg Scatter (ZDRBEBG) technique does not use information from the Melting Layer Detection Algorithm or the Hydrometeor Classification Algorithm, thus it can be influenced by other particles that have similar radar characteristics. In particular, ZDRBEBG seems most influenced by light winter precipitation. This results in a higher than expected ZDRBEBG value due to the non-zero $\text{ZDR}_{Intrinsic}$ value of the other particle types. Several statistical tests are included in the ZDRBEBG technique to avoid contamination from precipitation as well as biota. Results from Richardson et al. (2017a,b) show the filters adequately capture and eliminate the majority of contaminated estimates.

Results from each estimation method are used to make long-term tracks of ZDR Bias at a single radar site (Figure 1). Because many internal and external factors impact ZDR Bias, estimates taken from each volume scan go into the calculation for a daily median

* Corresponding author address: Lindsey M. Richardson, Radar Operations Center, Norman, OK, e-mail: Lindsey.M.Richardson@noaa.gov
AMS 39th ICRM

1

estimate of ZDR Bias for each estimation method. Such charts are used to assess sites with ZDR Bias beyond a recommended limit of ±0.2 dB. Correcting issues to bring ZDR Bias back within a recommended ±0.2 dB threshold mitigates potential errors in Quantitative Precipitation Estimation (QPE).

Unfortunately, the increased variance and chance of having a more positive bias from large drops and convection reduces the reliability of the current Light Rain method compared to the Dry Snow and Bragg Scatter methods. This leads to estimates from Light Rain being ignored entirely when their trend is different from ZDRBEDS and ZDRBEBG results. Figure 1 shows an example where users may ignore the Light Rain estimates because the ZDRBELR trend differs noticeably compared to Dry Snow and Bragg Scatter around the same timeframe. Questionable reliability introduces interpretation challenges when only estimates from Light Rain are available because of the difficulty of determining the existence of a ZDR Bias beyond potential estimation error. An improved method of estimating ZDR Bias from Light Rain is explored to reduce the variability of estimates and minimize estimation bias. For this study, Light Rain characteristics and related ZDR Bias estimation are considered using only non-derived products of Reflectivity (Z), Signal-to-Noise Ratio (SNR), Differential Reflectivity (ZDR), Correlation Coefficient (RHO), and Differential Phase (PHI). No information from derived products such as the MLDA or HCA is used in this study to avoid compounding potential errors from those products. As such, the authors admit the necessity for extra scrutiny in determining non-contaminated light rain returns in radar data.

2. FACTORS OF ESTIMATES FROM LIGHT RAIN

2.1 Tropical vs. Continental

Previous work has shown that the value of ZDR spreads with increasing reflectivity depending on the environment. Figure 2 (Figure 10 in Cao et al. 2008) shows Z vs. ZDR for rain data from disdrometers in Oklahoma and the estimated mean line from their other study in Florida (Zhang et al. 2001; Cao et al. 2006). Higher reflectivity values result in an increase in the expected ZDR based on the mean while also increasing the spread of possible ZDR observed in light rain. A mean continental trend at a higher ZDR values than the tropical trend relates to tropical environments more often have distributions of many small drops compared to the large drops developed during convective growth (e.g., Bringi et al. 2003).

The original ZDRBELR technique on the WSR-88D uses the intrinsic ZDR values for each specific Z category shown in Table 1. These roughly follow the mean line in Figure 2, yet the spread of ZDR values increases as dBZ increases. Estimating from Figure 2, the spread of data at 20 dBZ is from 0.0 up to 1.0 dB. By 25 dBZ the spread is from 0.0 up to 1.6 dB – at least 0.6 dB more spread than 20 dBZ. One option to reduce variance is to use only the lowest category with Z values between 19.0 and 21.0 dBZ. The mean $ZDR_{Intrinsic}$ values are between 0.23 and 0.27 dB; we opted to use 0.25 dB because it is between the cate-

gories and leans more towards the naturally higher dB values that could come from distribution contamination from larger drops. That is, using a slightly higher intrinsic value helps mitigate impacts from some larger drops.

TABLE 1. $ZDR_{Intrinsic}$ values associated with specific ranges of Z in the original ZDRBELR method.

Z (dBZ)	$ZDR_{Intrinsic}$ (dB)
19.0 – 20.5	0.23
21.0 – 22.5	0.27
23.0 – 24.5	0.32
25.0 – 26.5	0.38
27.0 – 28.5	0.46
29.0 – 30.5	0.55

2.2 Base Data Filters

All radar range gates with Reflectivity values between 19.0 and 21.0 dBZ can be collected as part of a statistical sample set for estimating ZDR Bias, but reflectivity alone does not convey the cleanliness or adequacy of making an estimate from the return. Returns could be contaminated by ground clutter signals, biota, other meteorological particles, or down-radial attenuation.

Signal-to-Noise Ratio (SNR) can be used to ensure returns are adequate enough signal to use for estimation of ZDR Bias. Requiring SNR above 20 dB matches the existing ZDRBELR and ZDRBEDS techniques. The threshold is carried through in this study as a metric for accumulating data for statistics.

Requiring Correlation Coefficient (RHO) to exceed 0.98 is another existing threshold of the ZDRBELR and ZDRBEDS methods. Lower correlation coefficient values often correspond with ground clutter, biota, or mixed return types. A uniform distribution is desired for the estimation of ZDR Bias from light rain due to the large variability of the $ZDR_{Intrinsic}$ value between particle types and sizes.

A range limit of 10 to 250 km (~5 to 135 nmi) can be used to avoid near-radar ground clutter and reduce the chance for encountering the melting layer and potential ice crystals. This range limit could be extended if using information from derived products such as the Melting Layer Detection Algorithm, which are not being used in this study to avoid compounding errors from derived products. The narrow range limit from 10 to 250 km coupled with an elevation angle limitation can mitigate impacts from ground clutter with the lower limit and ice crystal contamination with the upper limit. Elevation angles less than 1.8° were selected to pair with the range limits to keep below the melting layer as much as possible without additional outside information.

Winter weather conditions can overcome the elevation, range, and RHO filters suggested above because snow and ice crystals often have the same characteristics as light rain in radar data. Areas of melting snow around the melting layer would not pass the RHO filter, so major impacts from regions of large, wet drops will not pass through the filters. Impacts from nearby convection seeding clouds generating some large drops within a distribution of mostly small-

er drops would also be missed with these filters and could impact bias estimation. Because these base filters cannot overcome winter weather and some convective influences, other statistical tests may be used to distinguish which range gates should be used for ZDR Bias estimation.

3. TRAINING DATA SET

3.1 *Site/Time Selection*

To determine statistical filters that could be used for ZDRBELR, cases determined to be light rain must be explored for their statistical metrics. Comparisons are made with other influences such as convection, winter weather, and biota/clutter. Training data should therefore span a sufficient amount of time to capture the chance for winter weather and convection such as a full year. A timeframe from July 2016 through July 2017 covers this well and can be assessed quickly using shade charts such as the example shown in Figure 1. We selected a set of sites to be used for a training data set using the following criteria based on the shade charts:

1) The relative ZDR Bias trend between the three external target methods must be relatively stable across the entire year. Sites with large changes related to known hardware changes that could impact ZDR Bias are excluded to avoid contaminating the data set.
2) Sites with a ZDR Bias trend close to 0.0 dB were preferred. Sites with bias are allowed, but the bias must be accounted for when used in the training data set.
3) Sites with ZDRBELR values notably different from ZDRBEDS and ZDRBEBG were separated out for use in the verification data set. Sites with ZDRBELR close to the other target trends were key candidates for the training data set.
4) The site must have ZDRBELR values for over half of the year to be relevant for the training data set which needs as much data as possible across different seasons of the single year.
5) WSR-88D sites with multi-transmitter configurations were excluded from the training and verification data set to avoid complications of mixing information from the different configurations. Each hardware chain has a unique ZDR Bias that can be difficult to isolate in a bulk statistic without meticulous calculations beyond the scope of this study.

Figure 3 shows examples of 6-month shade charts and their relation to the criteria above.

A set of 24 sites were selected to be used to determine what the radar views as Light Rain targets (Figure 4 and Table 2). The sites cover a range of geographical environments, yet geographical spread was not used as a criterion for selection. A grouping of sites along the Northern Mississippi River Valley was pure chance that may be related to the weather events and environment seen specifically between July 2016 and July 2017.

Four sample months in this timeframe were used to get a sample of statistical metrics: July 2016, October 2016, January 2017, and April 2017. For each month, the monthly estimated ZDR Bias was applied as a correction factor to ZDR values for the given site to place the values closer to natural, unbiased ZDR to more accurately calculate statistical metrics that relate to light rain targets. The monthly value used for each site is listed in Table 2.

TABLE 2. Training Data Set WSR-88D sites and their monthly ZDR Bias Estimate correction factor.

| Site | Location | Monthly ZDR Bias Estimate | | | |
		Jul 2016	Oct 2016	Jan 2017	Apr 2017
KAPX	Gaylord, MI	+0.08	+0.02	+0.10	+0.09
KBHX	Eureka, CA	-0.36	-0.08	-0.08	-0.12
KBOX	Boston, MA	+0.11	-0.03	-0.03	-0.08
KBRO	Brownsville, TX	+0.07	-0.05	-0.11	-0.07
KCBW	Caribou, ME	+0.12	+0.05	-0.05	+0.06
KCXX	Burlington, VT	+0.06	-0.03	+0.01	+0.05
KDGX	Jackson, MS	+0.24	+0.01	-0.07	+0.00
KDVN	Quad Cities, IA	+0.10	+0.06	+0.06	+0.08
KEMX	Tucson, AZ	-0.10	-0.18	-0.15	-0.04
KEYX	Edwards AFB, CA	+0.29	-0.06	-0.06	-0.07
KFWS	Fort Worth, TX	-0.09	+0.04	-0.11	-0.06
KHTX	Huntsville, AL	+0.10	-0.06	-0.08	+0.07
KILX	Lincoln, IL	+0.05	-0.02	-0.01	+0.01
KLSX	St. Louis, MO	-0.04	-0.05	-0.02	+0.00
KLWX	Sterling, VA	+0.04	+0.02	+0.04	+0.02
KMKX	Milwaukee, WI	+0.10	+0.07	+0.11	+0.07
KPAH	Paducah, KY	+0.00	-0.04	-0.06	+0.00
KPDT	Pendleton, OR	-0.02	-0.08	-0.08	-0.06
KPUX	Pueblo, CO	+0.09	-0.04	+0.00	+0.02
KSHV	Shreveport, LA	+0.12	+0.13	+0.11	+0.13
KTLH	Tallahassee, FL	-0.03	-0.11	+0.08	+0.16
KTLX	Oklahoma City, OK	-0.02	+0.07	+0.04	+0.07
KUDX	Rapid City, SD	-0.04	-0.14	-0.10	-0.10
KVNX	Vance AFB, OK	+0.04	+0.13	+0.00	+0.03

Each volume scan from the site in the given month was processed using MATLAB 2017b with the base filters previously mentioned above applied to each applicable elevation scan:

- Elevation Angle < 1.8°
- 10 km < Range < 250 km
- 19.0 < Z < 21.0 dBZ
- SNR > 20 dB
- RHO > 0.98.

Radar range gates that pass the above filters were accumulated into histograms of ZDR, RHO and PHI. Each histogram used categories of their natural data resolution, so the full data set of actual values could be pulled out of the histogram if needed. Grouping of categories at values larger than the natural resolution could skew statistical metrics needed for distinguishing between return types. The mode of the resulting ZDR histogram was reported for each volume to be used for outlier analysis later.

A separate histogram of Z was collected that only uses the elevation and range limit. The wider range allowance of Z data will be used to assess the overall environment beyond the Z-filter limits used for ZDR Bias estimation. Categories range from -32.0 to 40.0 dBZ in 0.5 dBZ increments (the natural resolution of Z). Values of 40 dBZ and above are generally related to convection, so any histograms with high counts in this category are more likely to have influences from convection due to our use of a category cap.

Because the existing external target techniques accumulate information per volume scan and combine

these data into an estimate for a single day, an average of each metric from all volume scans in a given day were reported. Thus, the definition of a "Case" in this study relates to a single date in relation to 00 through 24 UTC. Cases do not span multiple days even in the larger meteorological event crosses dates. This ensures we can compare our existing daily metrics to daily cases.

3.2 *Visual Confirmation of Cases*

All days with metrics that pass the base filters with resulting statistical metrics were analyzed visually to classify the event type into one of four groups:

- Light Rain: Returns between 10 and 250 km have no reflectivity values above 45 dBZ anywhere in the domain, and dual-polarimetric variables have high correlation and relatively similar PHI and ZDR values without signs of mixed particle types or heavy attenuation.
- Convection: High reflectivity values and structures associated with convective influences. This may include signs of attenuation and mixed particle types such as rain and hail or different sizes of rain drops across a non-uniform Drop Size Distribution.
- Winter Weather: Signs of the melting layer or winter precipitation types anywhere within the 10 to 250 km limit. Many of these cases include Rain and Snow events that could be used for estimation hydrometeorological identification algorithms selected rain-specific bins. For our study without such data, we used the extreme approach to avoid all potential contaminants and strictly classify all cases with any chance of winter weather influence as Winter Weather cases.
- Clutter/Biota: Cases with most visible returns from Anomalous Propagation, Ground Clutter, interference or biological targets (e.g., birds or bugs).

Figure 5 displays an example of each Case classification. Images only go out to 150 km (~80 nmi) instead of 250 km for closer analysis of features in the example images. Textures of the returns, dual-polarimetric signatures, and reflectivity values quickly help determine the classification of a case. Some cases, especially Winter Weather cases, required additional verification from temperature and sounding records for complete confidence in the classification.

A total of 270 cases were visually inspected for return types over the given day. If any potential returns able to pass the filter were possibly contaminated, the cases were strictly placed in the classification with the possible contaminant. 153 cases had the potential for Convection, and 66 cases had potential impacts from Winter Weather. These cases may have significant areas of Light Rain within the 10-250 km range, but we are using the strict rules in this study to avoid estimation error. A total of 40 cases visually passed to be considered Light Rain, and only 6 cases were classified as Clutter/Biota because the Base Filters remove most of these already. Next, statistical metrics are used to determine characteristics of each category.

3.3 *Statistical Metrics*

Outliers can be defined as a certain deviation away from a mean value. If an accurate long-term trend is the focus, a monthly mean can be used as a metric for determining outliers of daily cases. For each month at each site, the mean of daily ZDR mode estimates was used to calculate a monthly mean. Each daily case ZDR mode was then compared to the monthly mean for determination of outlier cases. We chose the standard statistical definition, ±2 standard deviations away from the monthly mean, to mark a case as an outlier.

The classification of outlier/non-outlier for each case assists with testing of statistical filters to capture cases of Light Rain while avoiding cases with potential contaminants. Some cases of Convection and Winter Weather pass as non-outliers, which may be related to the strict rules we used for filtering. That is, the cases that pass as non-outliers may be mostly light rain with a small amount of potential contamination in the same viewing region.

The Bragg Scatter technique development revealed that the 90th Percentile of Z (Z90th) shown in Figure 6 (Figure 3 in Richardson et al. 2017a) exhibits a clear distinction between Bragg Scatter and precipitation. Additionally, the test of Inter-Quartile Range (IQR) is a useful filter for distributions with contamination such as biota or ground clutter. Such metrics could be refined for distinguishing light rain distributions from those with other target types or contamination. The following metrics were calculated for each volume scan for analysis:

- The total count of range gates accumulated in the ZDR histogram: ZDR_{Count}
- The IQR of ZDR: ZDR_{IQR}
- The Median Absolute Deviation around the median (MEDAD) of ZDR: ZDR_{MEDAD}
- The 90th Percentile of Z: Z90th
- The IQR of Z: Z_{IQR}
- The MEDAD of Z: Z_{MEDAD}
- The IQR of RHO: RHO_{IQR}
- The MEDAD of RHO: RHO_{MEDAD}
- The IQR of PHI: PHI_{IQR}
- The MEDAD of PHI: PHI_{MEDAD}

One may notice that almost all of the metrics listed are related to a spread test. Focus was put on spread metrics because contaminants combined with light rain returns cause more spread in the distribution and resulting histogram. This focus ties back to a leading goal of the study to mitigate variability of ZDRBELR values.

Metrics were compared via density plots to determine if any relationships existed to clearly define light rain samples. Each of the comparison metrics encompasses data for a single month of interest – data were not combined across the four focus months. Figure 7 shows an example relationship between the estimated ZDR mode based on the ZDR histogram in relation to the ZDR_{IQR}. The following

calculations were used to threshold results for clearer focus of interest regions:

Count Threshold = max (range gate count)/3   (2)
Other Metrics Threshold = max(metric)/2.   (3)

A division of three is used for the total count threshold because of the large overall number achievable compared to other metrics. All other metrics can sufficiently use a division of 2 to focus on a region of a density plot (Figure 7c and d).

Light rain metrics for KVNX in July 2016 shown in Figure 7 fall between 0.20 and 0.50 dB of ZDR based on the ZDR mode. This matches very closely with the distribution from the disdrometer study in Figure 2, which gives confidence to the effectiveness of the chosen Base Filters. Estimates correspond with a ZDR_{IQR} between 0.50 and 0.75 dB for this site month combination. With a natural resolution of 0.0625 dB, this relates to a spread of at least 8 categories up to 12 categories. A more narrow spread in the histogram could be related to a different return type, such as winter weather, while a broader spread could be related to influences from biota or convection.

These metrics were also compared to the classification determined by visual analysis. Exploration of the statistical metrics revealed that certain metrics had no strength at distinguishing Light Rain from other cases. The ZDR_{Count} filter is effective for avoiding cases marked as Biota/Clutter. Both RHO_{IQR} and RHO_{MEDAD} had no strength in filtering Light Rain from other classes. It is suspected this is in relation to the existing Base Filter specifying all RHO values must exceed 0.98. As such, the spread of RHO will always be narrow when considering values between 0.98 and the maximum of 1.05. For PHI, the IQR was effective at eliminating Convection cases, but the MEDAD has no strengths as a filter.

Z90th between 15.0 and 27.0 dBZ worked well even though overlap with other precipitation types is likely on the ends. Z_{IQR} between 12.0 and 18.0 were effective for eliminating many Winter Weather and Convection cases. Z_{MEDAD} had no additional benefit compared to using the $Z_{IQR.}$

ZDR had most benefit when using both the IQR and MEDAD as filters to keep Light Rain cases. The combination is effective for filtering out Winter Weather Cases at the low end and Convection at the high end. ZDR_{IQR} ranges from 0.5 to 0.70 dB worked well for Light Rain, while ZDR_{MEDAD} ranged from 0.200 and 0.375 dB.

Table 3 shows the total number of cases by category that pass when using specific statistical filters. Cases are broken into groups considered Outliers and Non-outliers as mentioned previously. The goal of keeping more non-outlier cases, and prioritizing the ones classified as Light Rain, presents challenges due to significant overlap of characteristics. Reducing non-outlier Convection and Winter Weather cases often impacted Light Rain as well. Thus, only ~37% of the cases classified as Light Rain pass the statistical filters. On the other hand, almost all outlier cases are effectively removed with statistical filters applied.

TABLE 3. Cases categorized by visual analysis in the Training Data Set and the remaining percentage of cases after applying suggested filters.

	Sum	Filtered Sum	%
Non-Outlier Light Rain	40	15	37%
Non-Outlier Convection	95	13	14%
Non-Outlier Winter Weather	44	3	20%
Outlier Clutter/Biota	6	0	0%
Outlier Convection	63	8	13%
Outlier Winter Weather	22	2	9%

Balancing the number of Light Rain cases kept with certain filter limits while reducing all other types of cases proved most challenging with the Winter Weather cases. Recall that Winter Weather cases include cases with light rain and winter precipitation targets. Thus, it is expected that the statistical metrics would still struggle with such cases. The statistical filters could be selecting cases with lower impacts from winter precipitation targets, but detailed analysis of that scale for each case is beyond the scope of this study.

3.4 Recommended Algorithm

During review of cases and metrics, other radar experts strongly suggested that the base filter be limited to a range of 150 km instead of 250 km. The authors accepted the suggestion as part of the verification data set to mitigate concerns about influence from frozen particles aloft. Ultimately, the following is recommended for ZDR Bias Estimation from Light Rain:

Step 1) Filters per Elevation Sweep
- Elevation Angle < 1.8°
- 10 km < Range < 150 km
- 19.0 < Z < 21.0 dBZ
- SNR > 20 dB
- RHO > 0.98

Step 2) Statistical Filters per Volume
- ZDR_{Count} > 600
- 0.50 <= ZDR_{IQR} <= 0.70 dB
- 0.200 <= ZDR_{MEDAD} <= 0.375 dB
- 15.0 <= Z90th <= 27.0 dBZ
- 12.0 <= Z_{IQR} <= 18.0 dB
- 0.3 <= PHI_{IQR} <= 6.0 degrees

Step 3) Calculate the mode of the ZDR histogram if it passes the filters from step 2.

4. VERIFICATION DATA SET

4.1 Site Selection

Similar to the Training data set, the Verification data set sites follow the criteria described in Section 3.1. The site must have ZDRBELR values at least half of the time of interest and cannot have a large change in the ZDR Bias trend related to known hardware changes/errors. The trend of ZDR Bias estimated from rain with the original method should be notably different from the trend seen with Dry Snow or Bragg Scatter methods. Sites with a positive-value ZDR-BELR trend when the ZDRBEDS and ZDRBEBG

show negative-value trends are prime candidates for testing if the new method overcomes the natural high bias from the original method.

Sites selected for the Verification data set will not be any sites used in the Training data set if using the previously-defined criteria. A separate set of 15 sites were selected to be used for a Verification data set (Figure 8 and Table 4). Again, geographical regions were not considered as part of site selection. The grouping of sites in the Southern Plains is likely related to the region receiving more precipitation from maritime air masses coupled with convective processes between July 2016 and July 2017.

TABLE 4. List of Verification Data Set WSR-88Ds.

Site	Location
KAMA	Amarillo, TX
KBGM	Binghamton, NY
KDDC	Dodge City, KS
KFDR	Altus AFB, OK
KGRB	Green Bay, WI
KICT	Wichita, KS
KINX	Tulsa, OK
KIWX	North Webster, IN
KMAF	Midland/Odessa, TX
KMPX	Minneapolis, MN
KOHX	Nashville, TN
KPBZ	Pittsburgh, PA
KRLX	Charleston, WV
KSGF	Springfield, MO
KTWX	Topeka, KS

Four focus months across the year were used for training, yet such a selection cannot be easily compared to a long-term trend like the 6-month shade chart. We chose to use the timeframe from February 2017 through July 2017 as the Verification set for comparison with long-term trends. This timeframe allows the new ZDRBELR method to be tested with extremes of Winter Weather cases early that transition to more cases with Clutter/Biota and Convection during the end of the timeframe. Additionally, spring months are often the most active weather months across the Contiguous United States, so the timeframe will ensure we are testing the method under some of the most difficult conditions available.

Each volume scan from the 15 sites was processed using the algorithm in Section 3.4 for the six months of February 2017 through July 2017. To match the process of the Dry Snow, and Bragg Scatter routine, volume-based calculations of the ZDR mode are used to calculation the ZDR Bias using equation (1). A $ZDR_{Intrinsic}$ value of 0.25 dB is used for all ZDRBELR values in this study as mentioned previously. The resulting ZDR Bias estimates for each volume go into a calculation for a median daily estimate, the points on the shade charts.

4.2 Visual Trend Comparison

Shade charts quickly give an overview of how the ZDRBELR method changes impact the long-term trend of ZDR Bias for given site. Comparisons of the new method and the original method from four of the Verification set sites are discussed. Shade charts for the timeframe shown are specific to weather events solely from the timeframe and do not represent any-

thing about the site/location in terms of general ZDR Bias trend or climatology of weather received beyond that given timeframe.

Midland/Odessa, TX (KMAF) is located in a semi-arid region that manages to receive snow in the winter and a moderate amount of convective weather during warmer months. From February through July 2017, KMAF received multiple estimates of ZDR Bias from all three external target types (Figure 9). The system started out with a negative ZDR Bias (colored blue on the chart). A slow increase in ZDR Bias occurred in June as suggested by the Dry Snow and Bragg Scatter estimates. This trend is completely obscured by the original method but is apparent with the improved algorithm. Some outliers from the trend are still noticeable, such as the event around 15 June 2017. Contamination from convection is a likely candidate based on the timeframe. Detailed analysis of such outlier cases in terms of the meteorology are beyond the scope of the study here yet should be mentioned for potential studies in the future.

Trends from Springfield, MO (KSGF) based on ZDRBEDS and ZDRBEBG show a negative ZDR Bias at the site for the entire 6 month timeframe (Figure 10). Estimates from all three external target types are available throughout the time period, partially in response to the sites proclivity to receive precipitation from mid-latitude cyclones and slightly cooler temperatures reducing the biota coverage for a longer time throughout the year. Estimates from the original Light Rain method show several shading regions with positive ZDR Bias even though the two other metrics confirm a negative ZDR Bias value. Estimates and the overall trend from the new method for ZDRBELR match with the ZDRBEDS and ZDRBEBG data. Even small areas of change, such as around 14 March 2017 and 05 May 2017, match in moving to a slightly more positive ZDR Bias estimate before returning around the original value. It should be clarified that the exact estimation points and days on the chart are not expected to match because each estimation target type may occur at different times and use their own specific rules for estimating ZDR Bias.

Minneapolis, MN (KMPX) is located at latitude that receives winter precipitation for more months out of the year compared to KMAF and KSGF (Figure 11). This appears in the shade chart as there are few to no estimates from Light Rain until April 2017. Estimates from Light Rain for the rest of the timeframe have a more positive value than the estimates from Dry Snow and Bragg Scatter. The trend matches closely between all three methods with the improved Light Rain estimation, yet there are more estimates during the winter and early spring. This could be related to multiple variables, specifically potential cases of mixed precipitation with liquid and frozen particles. Additionally, the original method uses information from derived products unavailable to our processing scheme for this study. If information about the melting layer and hydrometeor classification were combined with the improved estimation technique, the number of winter weather events appearing as Light Rain would be expected to decrease.

Finally, an example from Dodge City, KS (KDDC) reveals a natural variation of ZDR Bias across the

timeframe unrelated to hardware changes (Figure 12). A positive ZDR Bias turns more negative around 23 March 2017 and moves back towards positive values around 24 May 2017. This trend is almost completely overcome by the large positive bias from the original method due. KDDC is located in the Central Plains part of the Contiguous United States and receives a significant amount of strong convection throughout the year. Convective influences creating larger drops within drop size distributions can result in such a positive bias as seen here. With the new technique, Light Rain estimates clearly match the trend seen with the Dry Snow and Bragg Scatter techniques. Additionally, the variability of estimates appears reduced even during times with an increased risk of influence from convection in May through July. The new technique does have the potential for increased cases of light rain and winter precipitation, but it is unclear how much influence frozen particles are having on each case. These cases could be used for future studies into details of contribution types.

4.3 *Estimated Rain Outliers*

Assessing the daily points to the monthly trend can distinguish differences between the new and original method with regards to accurately capturing Light Rain targets that can be used for estimating ZDR Bias. Valid targets of Light Rain are expected to have reduced standard deviation and a reduced magnitude and number of outliers. For each site/month, the standard deviation was computed (Figure 13a). The new method shows lower standard deviations for a majority of the site/month combinations. It should be noted that the singularly high value around index 20 is related to an estimate reaching the maximum ZDR value reported of +8.0 dB due to clutter/biota contamination. Both the new and original methods are susceptible to such errors, so the y-axis is scaled for better focus of differences (Figure 13b). A difference between the original and new methods more clearly shows the majority of site/month combinations have improved standard deviations as only a few values fall below 0.0 dB (Figure 14).

Comparing the total number of outliers must be done as a ratio or percentage because the requirements for creating an estimate means that some days with an estimate in one method will not have an estimate in the other. This is evidenced by the differing total number cases reported by the original and the new techniques. Another way to determine differences of method accuracy comes from comparing the magnitude of difference between the outliers and the mean. In effect, this is an estimate of the bias of estimates seen with each method type because a bias is a difference of the estimate from the mean. Shade charts suggest the rain methods will have a positive-valued bias.

Results in Table 5 reveal that the new method and original method have approximately the same percentage of outliers for the relatively small sample set, but the magnitude of outliers is approximately half when using the new method. Impacts of high variability naturally available in the estimates could reduce the chance of classifying a case as an outlier when

comparing rain to rain. High standard deviation values increase the range that must be exceeded to count as an outlier, thus the total number of outliers may be smaller than expected. Variability of the estimate can be compared using the Inter-Quartile Range of daily estimates over a given site/month. Lower spread as indicated by lower IQR values suggest the new method has less overall variability compared to the original method.

TABLE 5. Daily values of ZDRBELR compared to the monthly mean trend of ZDRBELR.

	Original	New
Total Days Assessed	2715	2715
Number of Events	993	1086
Number of Outliers	35	33
Percentage of Outliers	4	3
Average Bias (dB)	+0.42	+0.21
Average IQR of Estimates (dB)	0.22	0.15

Thus far we have only compared rain to rain, yet a goal of the study is to ensure the overall trend from the three external target methods is similar. Previous examples showed the existing similarity of trends between Dry Snow and Bragg Scatter techniques, and the shade chart examples suggest the new technique matches these more accurately. For quantification tests, mean values of the ZDRBEDS and ZDRBEBG daily estimates were calculated to represent the trend for each site/month. Daily estimates of ZDRBELR were compared to this Snow/Bragg trend for calculations of variability and outliers (Table 6). Immediately noticeable is the larger number of cases marked as an outlier compared to the Snow/Bragg trend. The total number of outliers and overall bias is smaller with the new method compared to the original method. This corresponds well with the shade chart examples showing a similar matching trend between all three external target methods. Some outlier cases are still present, but the percentage is reduced by more than half of the original outlier percentage.

TABLE 6. Daily values of ZDRBELR compared to the monthly mean trend based on ZDRBEDS and ZDRBEBG combined.

	Original	New
Total Days Assessed	2715	2715
Number of Events	993	1086
Number of Outliers	406	174
Percentage of Outliers	41	16
Average Bias (dB)	+0.35	+0.22

5. SUMMARY AND DISCUSSION

External targets of Light Rain, Dry Snow, and Bragg Scatter can be used to estimate ZDR Bias on weather radars using data collected from normal operational scans. This is a preferred method on systems that cannot vertically point or are limited by operational scan times that take additional time to do a separate vertically-pointed scan. Such methods on the WSR-88D systems are used to track the relative ZDR Bias over time frames spanning several months.

7

There are many times when the trend from the ZDR Bias Estimated from Light Rain does not match the ones for Dry Snow or Bragg Scatter. Generally the estimates from Light Rain can result in a higher than expected result due to contamination from other particles or differences in the drop-size distribution related to convective influences. These differences between target types decrease confidence in the existence of a ZDR Bias and overall assessment of the bias value. ZDRBELR values also showed more variability than other external targets and contributes to decreased confidence in the estimate.

Several steps were explored to reduce variability of the estimates from Light Rain while also reducing the high bias. The first step was reducing the set of Z values to a narrow region with a single $ZDR_{Intrinsic}$ value instead of a larger region with more natural variability. A $ZDR_{Intrinsic}$ value of 0.25 dB was selected to represent regions of light rain associated with the narrow Z limits. This value is close to previously suggested values of 0.23 and 0.27 dB and leans slightly more positive as a chance to mitigate chance of receiving a high bias estimate from a light rain distribution due to other particle types. Using a $ZDR_{Intrinsic}$ of 0.25 dB for light rain is only 0.05 dB higher than the value used for Dry Snow. As such, estimates from the Light Rain method that truly are dry snow instead would only have potential errors of 0.05 dB from the $ZDR_{Intrinsic}$ selection. This does not account for other estimation errors due to contents of the sampling distribution.

Base Filters on the data facilitate isolating radar range gate returns that are most likely to be related to light rain signatures. Information from the resulting Base Filter data set was used to create a Training Set using four months of data from 24 WSR-88D sites. Statistical metrics were explored for each set to determine if filters could be used to better isolated Light Rain events from cases with potential contamination from things such as frozen particles or convection that would introduce larger errors in the ZDR Bias estimate. Cases were visually analyzed by a team of radar experts and classified into categories of Light Rain, Winter Weather, Convection, and Clutter/Biota. Classifications used strict rules, so some cases have overlap that may pass statistical filter tests. A set of Statistical filters was found that keeps more Light Rain cases while reducing the number of contamination cases. These filters also reduce the number of cases marked as outliers and keep more non-outlier cases.

A new algorithm was proposed for ZDR Bias Estimation from Light Rain that accumulates data from individual elevation angles of a volume scan which are then used to calculate statistical metrics. If the data set passes the Statistical Filters, then a ZDR Bias value can be estimated from the data set with a higher confidence level. Six months of data from 15 separate WSR-88Ds served as a Verification Set. Results from the verification revealed trends that match more closely with ZDRBEDS and ZDRBEBG when using long-term trend shade charts. Furthermore, quantitative estimates of the number of variability, number of outliers, and magnitude of outliers show

improvement with the new method compared to the original metric.

The cases in this study are from a limited number of sites over a limited time frame that may not be representative of other time frames or locations. Calculations were the same for the original and new method, so the metrics should be justifiable with the caveat of the known time frame and potentially small sample size in both. Improvements seen with the small sample are significant enough to recommend using the new method as an operational ZDR Bias estimate compared to the original method.

Information from derived products such as hydrometeor classification or melting layer detection could be used to further reduce the chance of estimation error from other target types. Such additions would be required if the technique focused on higher elevation angles that are more likely to encounter the melting layer and frozen particles more quickly in range. Impacts of additional constraints could be explored in a future study or in an operational test environment with access to full products in real time.

ZDR Bias estimation is a challenge for all polarimetric weather radar systems. Many methods have been explored, and they all have unique caveats. Using multiple separate tests for estimating ZDR Bias is one way to increase confidence in the existence and reported value of a ZDR Bias. The improved method presented in this study shows promise as another technique to estimate ZDR Bias with a higher confidence level.

6. ACKNOWLEDGEMENTS

7. REFERENCES

Atlas, D., 1959: METEOROLOGICAL "ANGEL" ECHOES. *J. Meteor.*, **16**, 6–11, https://doi.org/10.1175/1520-0469(1959)016<0006:ME>2.0.CO;2.

Atlas, D., 2002: RADAR CALIBRATION. *Bull. Amer. Meteor. Soc.,* **83**, 1313–1316, https://doi.org/10.1175/1520-0477-83.9.1313.

Bechini, R., L. Baldini, R. Cremonini, and E. Gorgucci, 2008: Differential Reflectivity Calibration for Operational Radars. *J. Atmos. Oceanic Technol.,* **25**, 1542–1555, https://doi.org/10.1175/2008JTECHA1037.1.

Bechini, R., V. Chandrasekar, R. Cremonini, and S. Lim, 2010: Radome attenuation at X-band

radar operations. *Proc. Sixth European Conf. on Radar in Meteorology and Hydrology,* Sibiu, Romania, ERAD, P15.1.

Bringi, V.N., V. Chandrasekar, J. Hubbert, E. Gorgucci, W.L. Randeu, and M. Schoenhuber, 2003: Raindrop Size Distribution in Different Climatic Regimes from Disdrometer and Dual-Polarized Radar Analysis. *J. Atmos. Sci.*, **60**, 354–365, https://doi.org/10.1175/1520-0469(2003)060<0354:RSDIDC>2.0.CO;2.

Cao, Q., G. Zhang, T. Schuur, A. Ryzhkov, E. Brandes, and K. Ikeda, 2006: Characterization of rain microphysics based on disdrometer and polarimetric radar observations. *Proc. IGARSS* 2006, Denver, CO, IEEE, 02_11A05.

Cao, Q., G. Zhang, E. Brandes, T. Schuur, A. Ryzhkov, and K. Ikeda, 2008: Analysis of Video Disdrometer and Polarimetric Radar Data to Characterize Rain Microphysics in Oklahoma. *J. Appl. Meteor. Climatol.*, **47**, 2238–2255, https://doi.org/10.1175/2008JAMC1732.1.

Davison, J. L., R. M. Rauber, and L. Di Girolamo, 2013a: A Revised Conceptual Model of the Tropical Marine Boundary Layer. Part II: Detecting Relative Humidity Layers Using Bragg Scattering from S-Band Radar. *J. Atmos. Sci.*, **70**, 3025–3046, doi: https://doi.org/10.1175/JAS-D-12-0322.1.

Davison, J. L., R. M. Rauber, L. Di Girolamo, and M. A. LeMone, 2013b: A Revised Conceptual Model of the Tropical Marine Boundary Layer. Part III: Bragg Scattering Layer Statistical Properties. *J. Atmos. Sci.*, **70**, 3047-3062, doi: https://doi.org/10.1175/JAS-D-12-0323.1.

Gorgucci, E., G. Scarchilli, and V. Chandrasekar, 1992: Calibration of radars using polarimetric techniques.*IEEE Trans. Geosci. Remote Sens.*, **30,** 853–858, https://doi.org/10.1109/36.175319.

Hardy, K. R., and I. Katz, 1969: Probing the clear atmosphere with high power, high resolution radars. *Proc. IEEE*, **57**, 468–480, https://doi.org/10.1109/PROC.1969.7001.

Knight C.A. and L. J. Miller, 1998: Early radar echoes from small warm cumulus: Bragg and hydrometeor scattering. J. Atmos. Sci., 55, 2974-2992, https://doi.org/10.1175/1520-0469(1998)055<2974:EREFSW>2.0.CO;2.

McCormick, G. C., and A. Hendry, 1975: Principles for the radar determination of polarization properties of precipitation. *Radio Sci.*, **10**, 421-434, https://doi.org/10.1029/RS010i004p00421.

Meischner, P. F., V. N. Bringi, M. Hagen, and H. Höller, 1991: Multiparameter radar characterization of a melting layer compared with in situ measurements. Preprints, *25th Int. Conf. on Radar Meteorology*, Paris, France, Amer. Meteor. Soc., 721–724.

Melnikov, V. M., R. J. Doviak, D. S. Zrnić, and D.J. Stensrud, 2013a: Structures of Bragg Scatter Observed with the Polarimetric WSR-88D. *J. Atmos. Oceanic Technol.*, **30**, 1253–1258, https://doi.org/10.1175/JTECH-D-12-00210.1.

Melnikov, V., D. Zrnić, M. Schmidt, and R. Murnan, 2013b: ZDR calibration issues in the WSR-88Ds. Report on 2013-MOU, 54 pp. [Available online at: http://www.nssl.noaa.gov/publications/wsr88d_reports/WSR88D_ZDRcalib_Report_2013.pdf].

Richardson, L.M., J.G. Cunningham, W.D. Zittel, R.R. Lee, R.L. Ice, V.M. Melnikov, N.P. Hoban, and J.G. Gebauer, 2017a: Bragg Scatter Detection by the WSR-88D. Part I: Algorithm Development. *J. Atmos. Oceanic Technol.*, **34**, 465–478, https://doi.org/10.1175/JTECH-D-16-0030.1.

Richardson, L. M., W. D. Zittel, R. R. Lee, V. M. Melnikov, R. L. Ice, and J. G. Cunningham, 2017b: Bragg Scatter Detection by the WSR-88D. Part II: Assessment of ZDR Bias Estimation. *J. Atmos. Oceanic Technol.*, **34**, 479–493, https://doi.org/10.1175/JTECH-D-16-0031.1.

Ryzhkov, A. V., S. E. Giangrande, V. M. Melnikov, and T. J. Schuur, 2005: Calibration Issues of Dual-Polarization Radar Measurements. *J. Atmos. Oceanic Technol.,* **22**, 1138–1155, https://doi.org/10.1175/JTECH1772.1.

Schuur, T. J., A. V. Ryzhkov, and D. S. Zrnić, 2001: A statistical analysis of 2D-video-disdrometer data: Impact on polarimetric rainfall estimation. Preprints, *30th Int. Conf. on Radar Meteorology*, Munich, Germany, Amer. Meteor. Soc., 11B.4. [Available online at https://ams.confex.com/ams/30radar/techprogram/paper_21554.htm.]

Schuur, T.J, A.V. Ryzhkov, and D. R. Clabo, 2005: Climatological analysis of DSDs in Oklahoma as revealed by 2D-video disdrometer and polarimetric WSR-88D radar. *32nd Conf. on Radar Meteorology*, Albuquerque, NM, Amer. Meteor. Soc., 15R.4. [Available online at https://ams.confex.com/ams/32Rad11Meso/techprogram/paper_95995.htm.]

Seliga, T. A., V. N. Bringi, and H. H. Al-Khatib, 1979: Differential reflectivity measurements in rain: First experiments. *IEEE Trans. Geosci. Electron.*, **17**, 240–244, https://doi.org/10.1109/TGE.1979.294652.

Straka, J.M., D.S. Zrnić, and A.V. Ryzhkov, 2000: Bulk Hydrometeor Classification and Quantification Using Polarimetric Radar Data: Synthesis of Relations. *J. Appl. Meteor.*, **39**, 1341–1372, https://doi.org/10.1175/1520-0450(2000)039<1341:BHCAQU>2.0.CO;2.

Vivekanandan, J., G. Zhang, S. M. Ellis, D. Rajopadhyaya, and S. K. Avery, 2003: Radar reflectivity calibration using differential propagation phase measurement. *Radio Sci.*, **38**, 8049, doi: https://doi.org/10.1029/2002RS002676.

Wilks, D. S., 2006: Statistical Methods in the Atmospheric Sciences. 2nd Edition. International Geophysics Series, Vol. 91, Academic Press, 627 pp.

Williams, E. R., M. F. Donovan, D. J. Smalley, R. G. Hallowell, E. Griffin, K. T. Hood, and B. J. Bennett, 2015a: The 2013 Buffalo Area Icing and Radar Study (BAIRS). MIT Lincoln Lab. Rep. ATC-419, 132 pp.

Williams, E.R., D.J. Smalley, M.F. Donovan, R.G. Hallowell, K.T. Hood, B.J. Bennett, R. Evaristo, A. Stepanek, T. Bals-Elsholz, J. Cobb, J. Ritzman, A. Korolev, and M. Wolde, 2015b: Measurements of Differential Reflectivity in Snowstorms and Warm Season Stratiform Systems. *J. Appl. Meteor. Climatol.*, **54**, 573–595, https://doi.org/10.1175/JAMC-D-14-0020.1

Zhang, G., J. Vivekanandan and E. Brandes, 2001: A method for estimating rain rate and drop size distribution from polarimetric radar measurements. *IEEE Transactions on Geoscience and Remote Sensing*, **39** (4), 830-841, https://doi.org/10.1109/36.917906.

Zittel, W. D., J. G. Cunningham, R. R. Lee, L. M. Richardson, R. L. Ice, and V. M. Melnikov, 2014: Use of Hydrometeors, Bragg Scatter, and Sun Spikes to Determine System ZDR Biases in the WSR-88D Fleet, *8th European Conference on Radar in Meteorology and Hydrology.* [Available online at https://www.roc.noaa.gov/WSR88D/PublicDocs/Publications/132_Zittel.pdf].

Zittel, W. D., R. R. Lee, L. M. Richardson, J. G. Cunningham, J. A. Schultz, and R. L. Ice, 2015: Geographical and Seasonal Availability of Light Rain, Dry Snow, and Bragg Scatter to Estimate WSR-88D ZDR System Bias, *31st Conference on Environmental Information Processing Technologies*. [Available online at https://ams.confex.com/ams/95Annual/webprogram/Manuscript/Paper265374/Zittel_11_2_31stEIPT_ExtendedAbstract.pdf.]
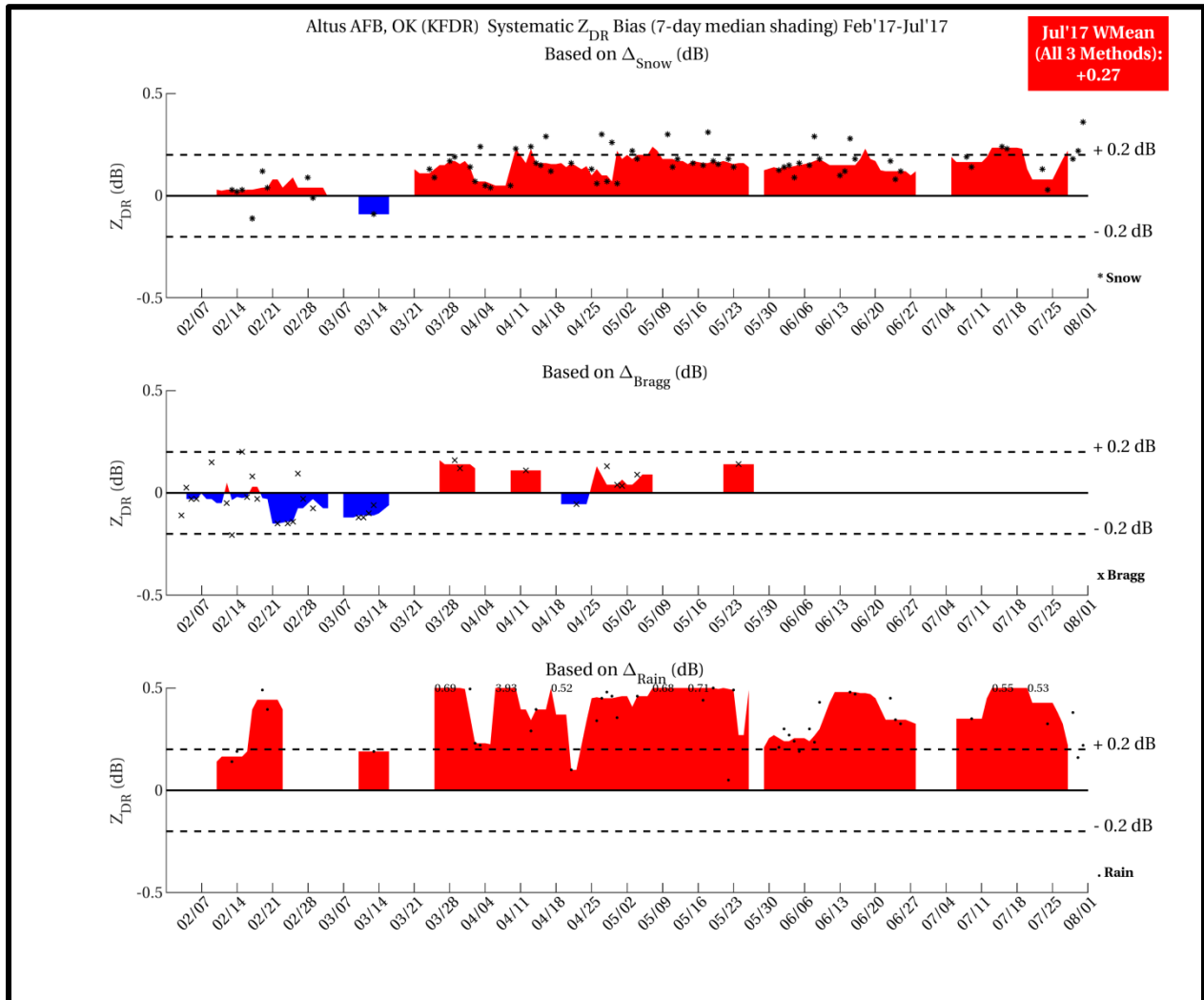
FIGURE 1. Example of a Shade Chart used to track ZDR Bias at a single WSR-88D site with estimates from Dry Snow (top panel), Bragg Scatter (middle panel), and Light Rain (bottom panel). The individual points in each panel represent the daily median ZDR Bias estimated from the given external target type. Shading is created by taking the 7 day median centered on the given date (i.e., using 3 before and 3 after). Information from all three external target methods are combined into a monthly weighted mean of the monthly median estimates. Weights are 0.42 for Bragg Scatter, 0.33 for Dry Snow, and 0.25 for Light Rain which roughly matches the order of least to most variability from the estimates. The weighted mean is a standard calculation on the chart but will not be discussed in detail in this study.
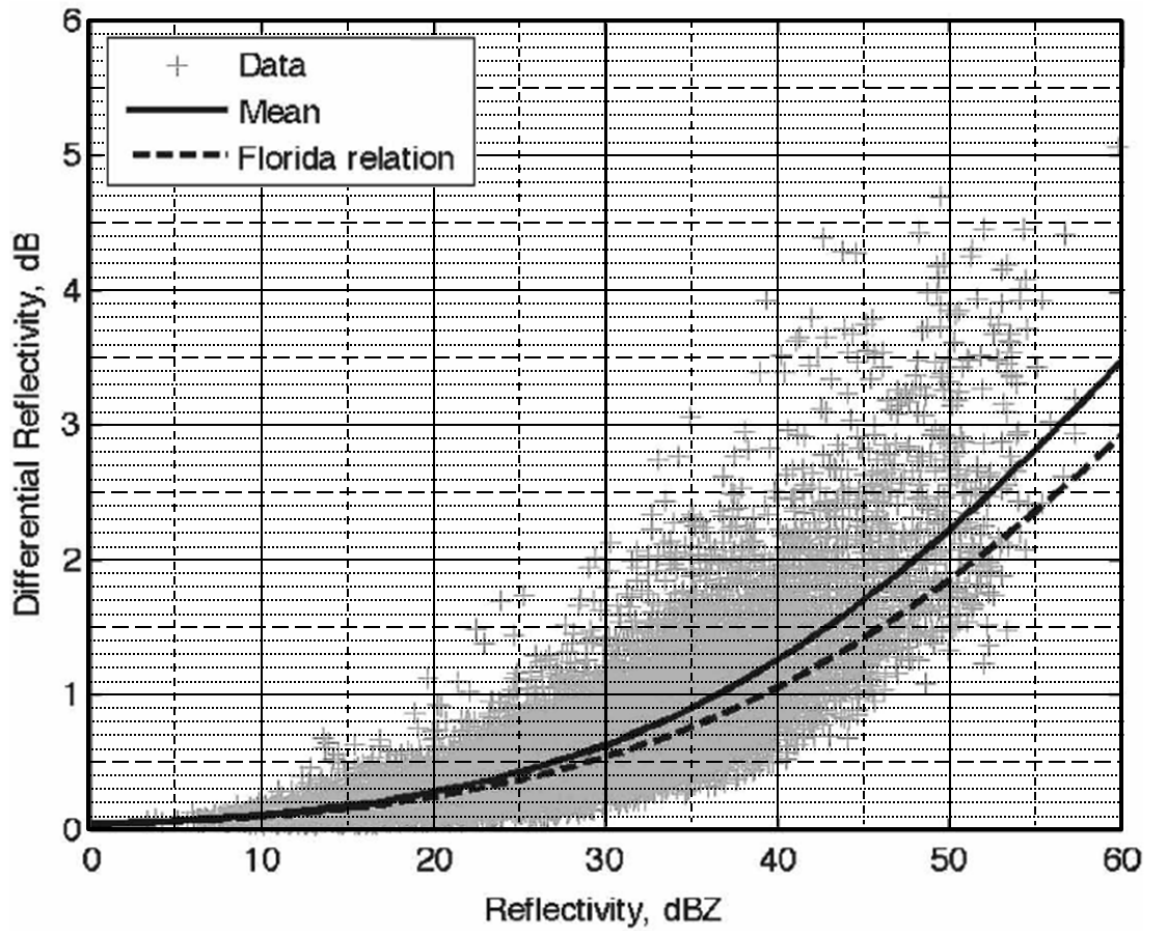
FIGURE 2. Originally Figure 10 in Cao et al. (2008), the plot of Z (dBZ) vs ZDR (dB) from disdrometer measurements in Oklahoma is shown here with additional axis lines to facilitate estimation of the total ZDR spread associated with specific Z categories. The solid line represents the mean relationship from the given disdrometer information while the dashed line represents the mean relationship seen from data collected in Florida.
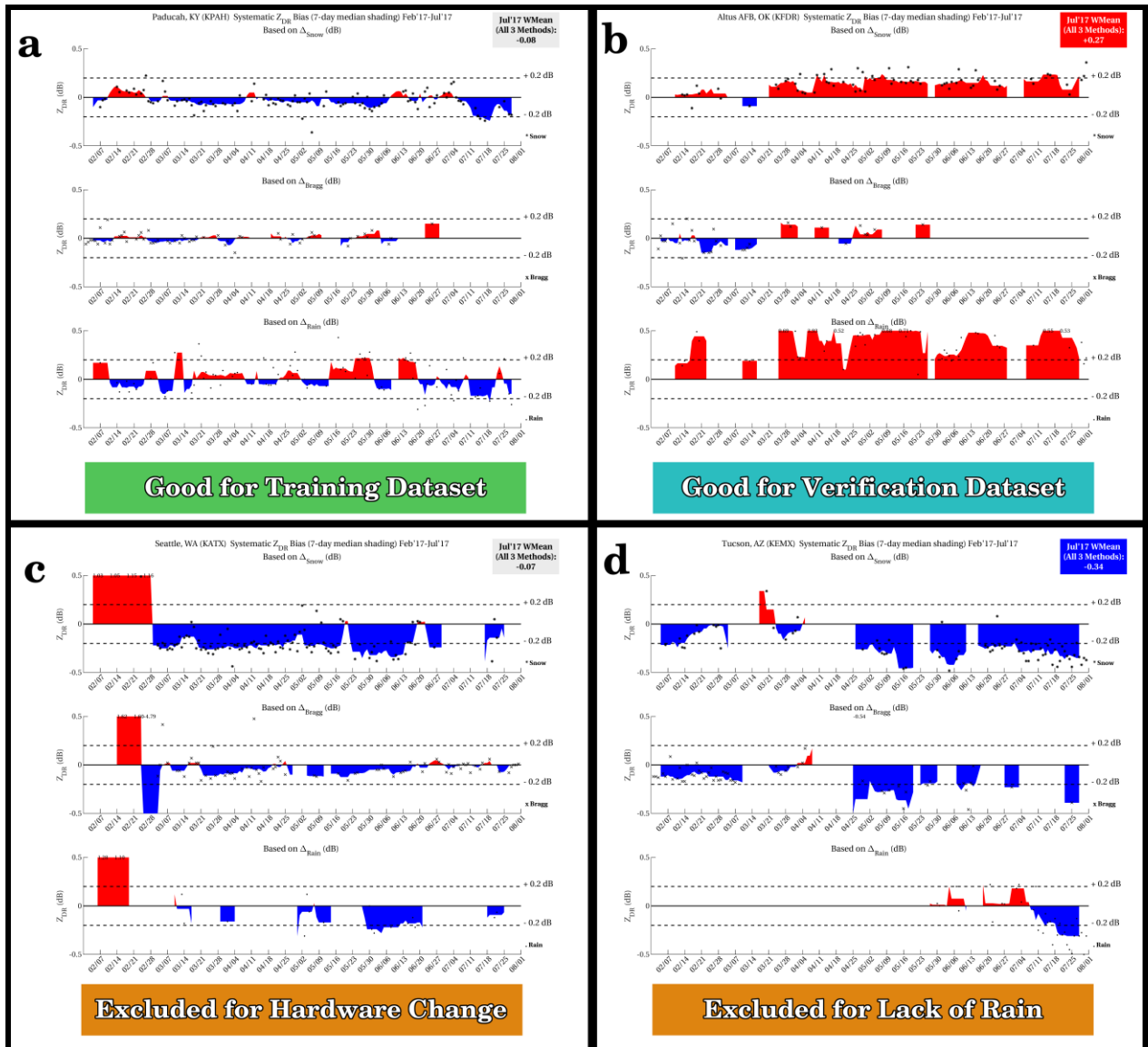
FIGURE 3. Examples of shade charts categorized into potential usefulness as a training data set or verification data set point using the criteria in Section 3.1.

FIGURE 4. Map showing the locations of WSR-88D sites with Training data set sites circled in green.
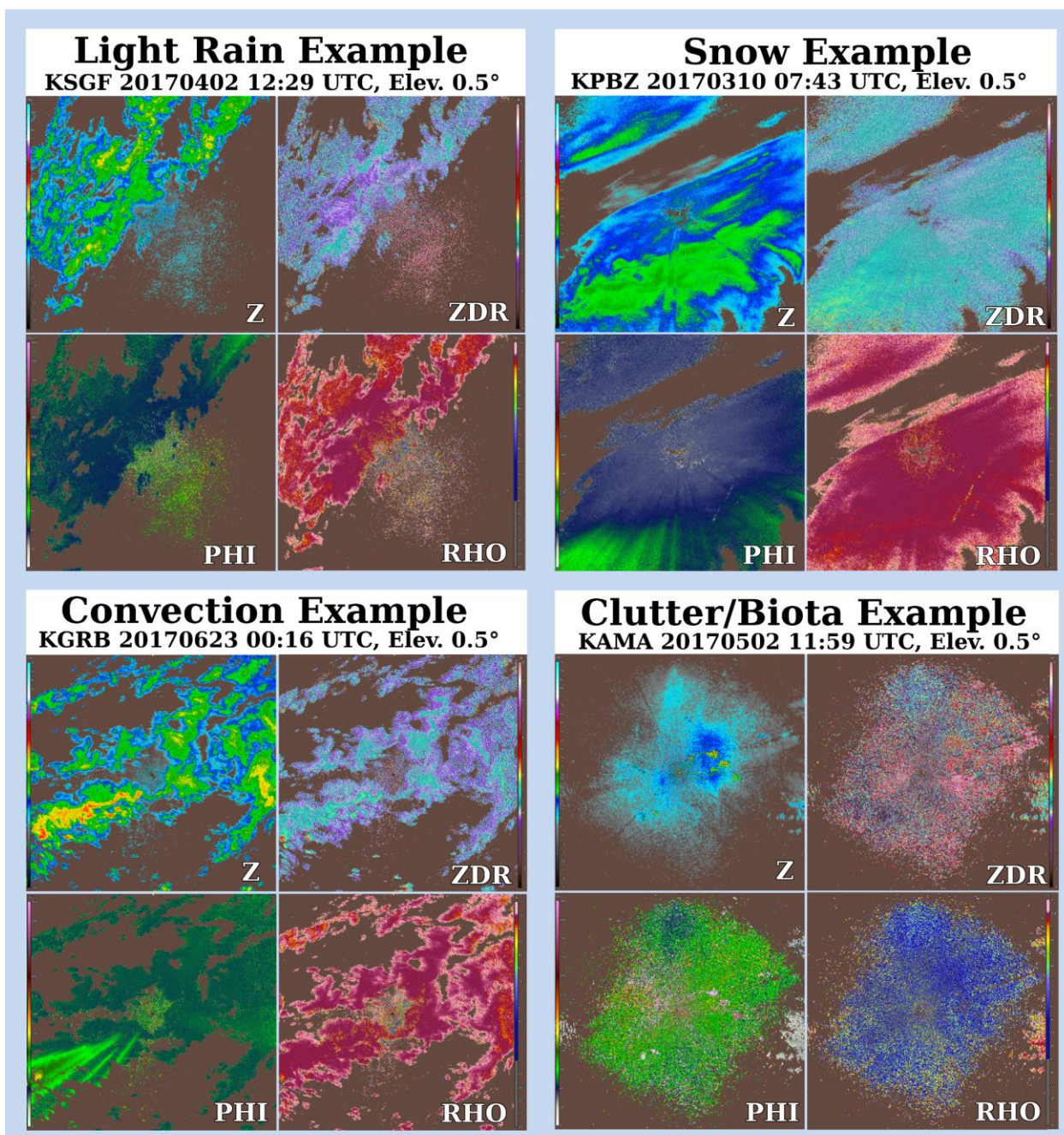
FIGURE 5. Samples of scans classified into specific types of cases described in section 3.2. Each Example is centered on the radar location and shows information out to 150 km (~80 nmi) in range.
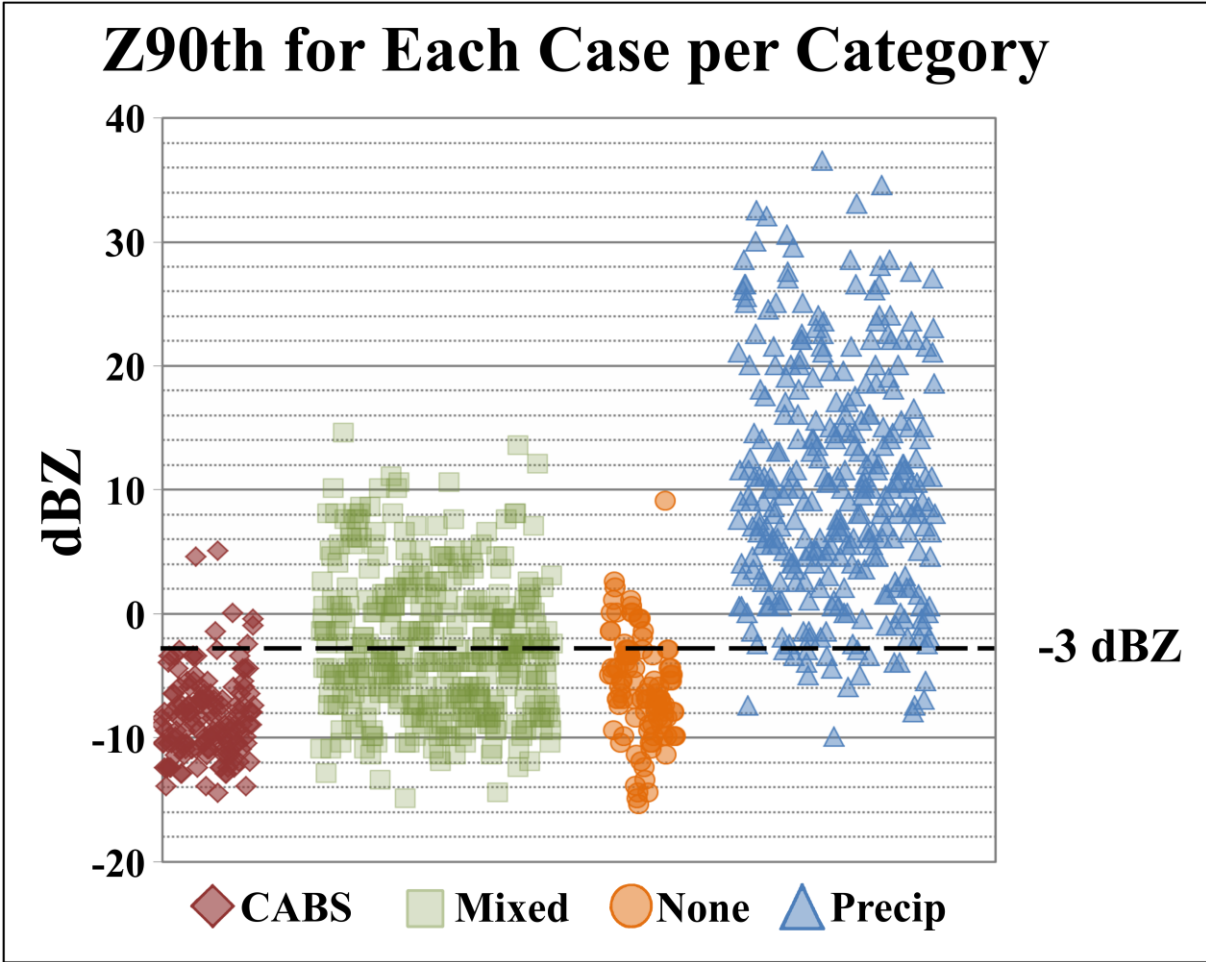
FIGURE 6. Originally Figure 3 in Richardson et al. 2017a, the resulting values of the 90th Percentile of Z classified via visual inspection show distinct levels between Clear Air Bragg Scatter (CABS), Mixed cases with Bragg Scatter and precipitation, None (Clutter/Biota), and Precipitation. Precipitation could be rain or winter weather returns, so the graphic here cannot be used explicitly as a test threshold in the Light Rain study. A similar technique is explored to determine filters for ZDRBELR.
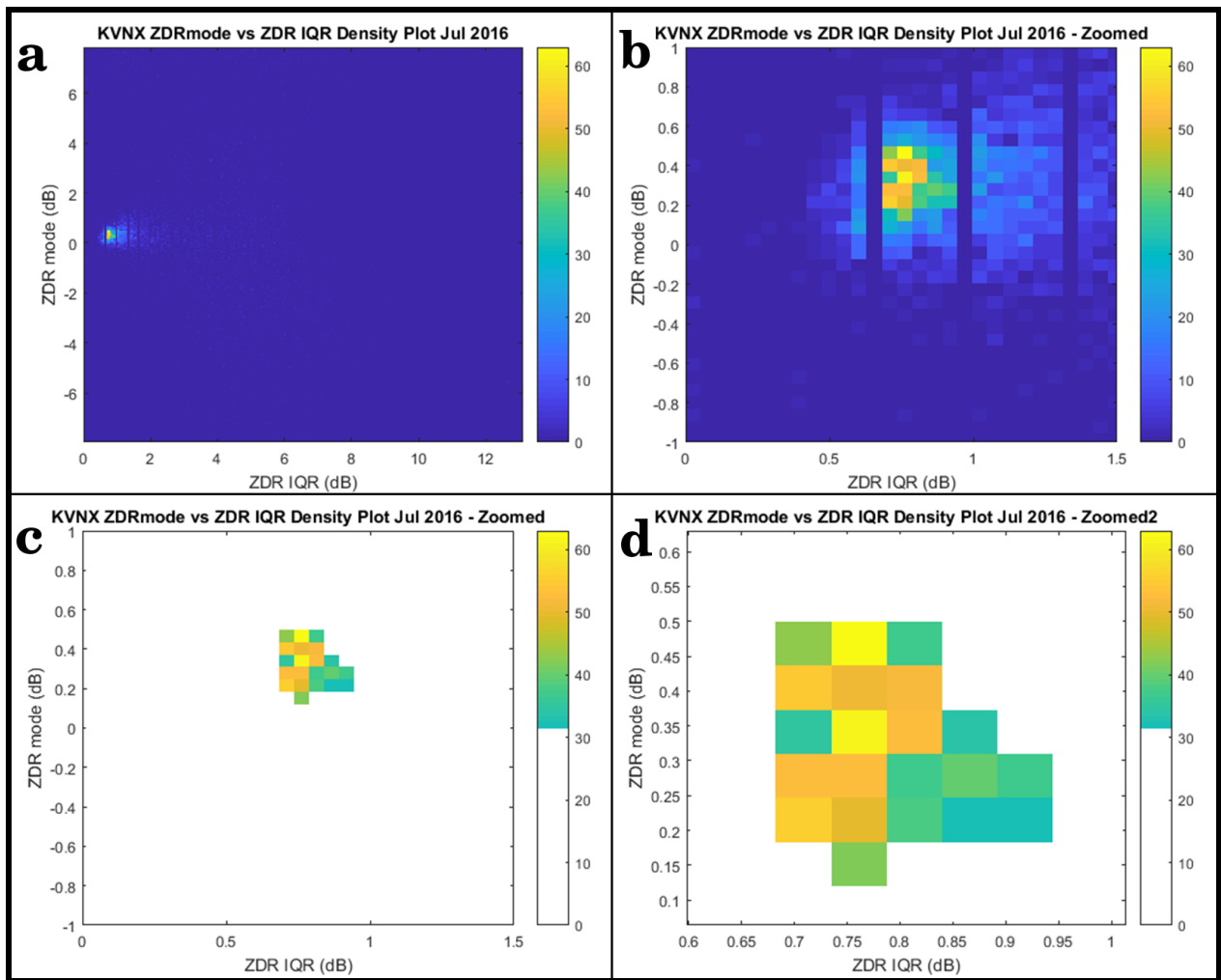
FIGURE 7. Density plot comparing the mode of ZDR points passing the Base Filters to the IQR of the same data from Vance AFB, OK (KVNX) during July 2016. (a) The full range of possible values. (b) Axes ranges are limited to focus on the region of most returns. (c) The same axes limits as (b) but only shows the values remaining after the threshold calculation of Equation (3). (d) Further limitation of the axes to assess fine-scale limits for this particular site/month combination.
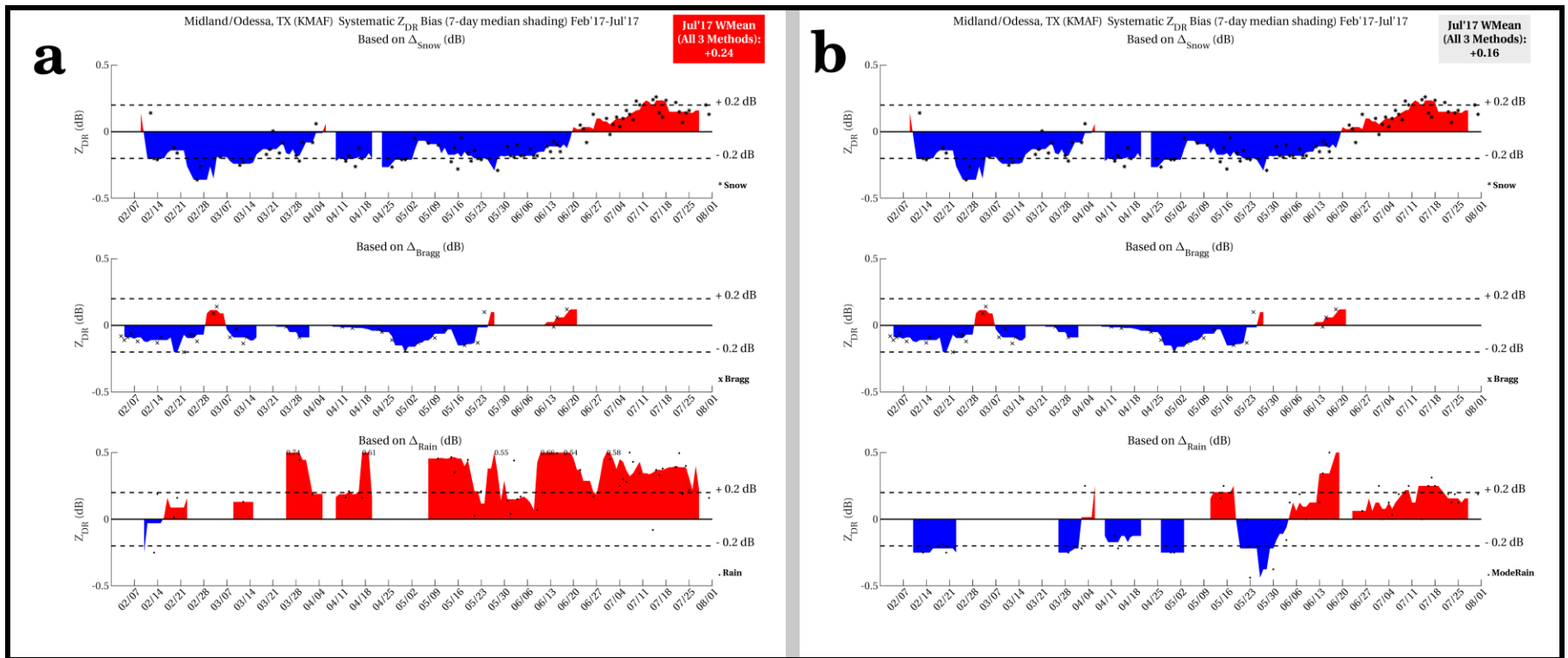
FIGURE 8. Map of WSR-88D sites with Verification data set locations circled in blue.

FIGURE 9. Shade chart with data from the (a) Original and (b) New ZDRBELR methods from Midland/Odessa, TX (KMAF). The information from the Dry Snow and Bragg Scatter techniques are the same in each image as they were unchanged in relation to the Light Rain test.
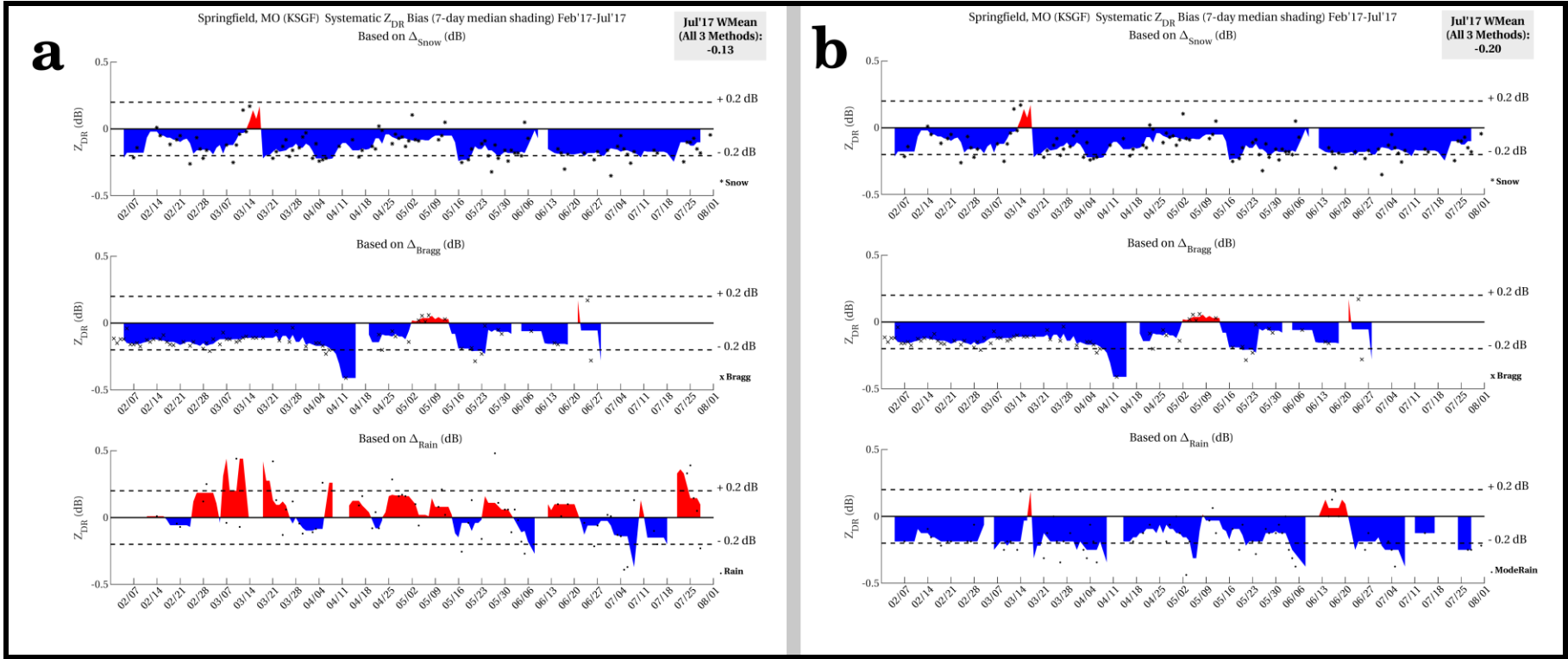
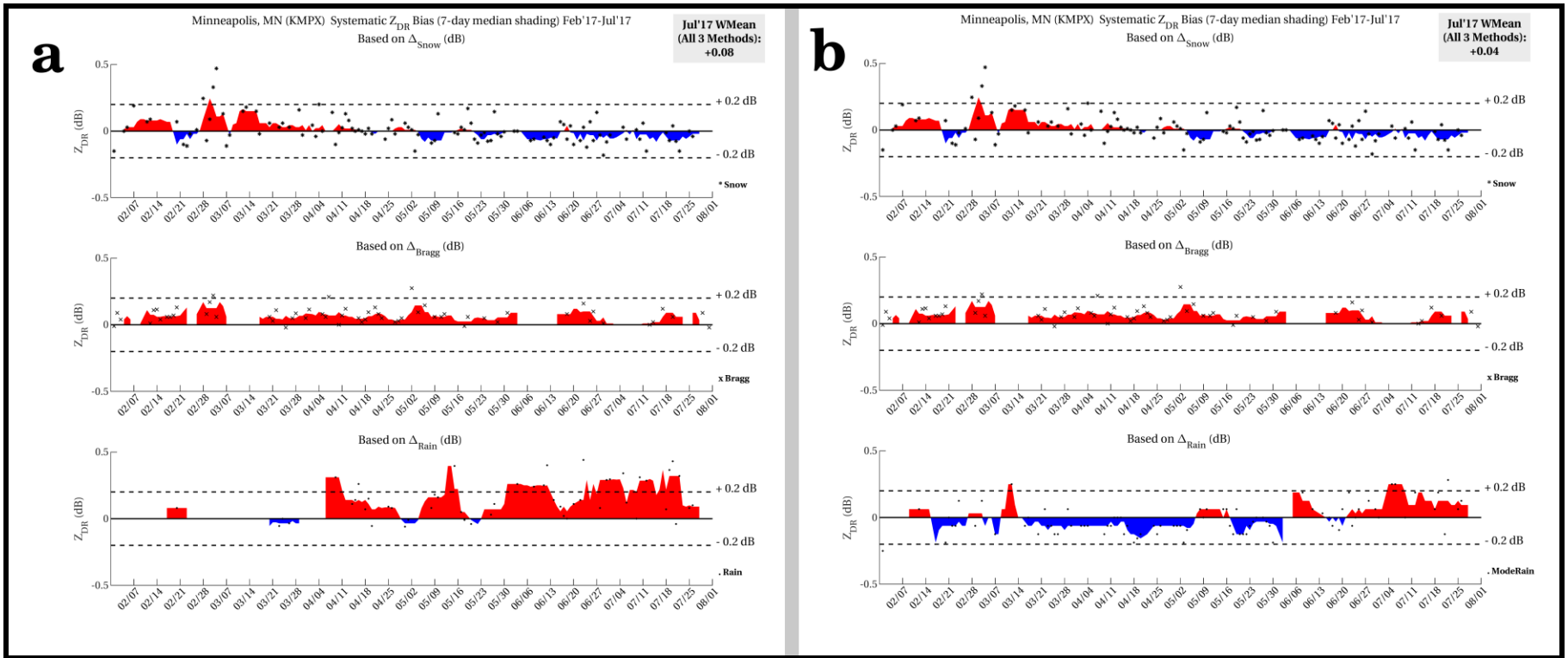FIGURE 10. Same as Figure 9 but for Springfield, MO (KSGF).

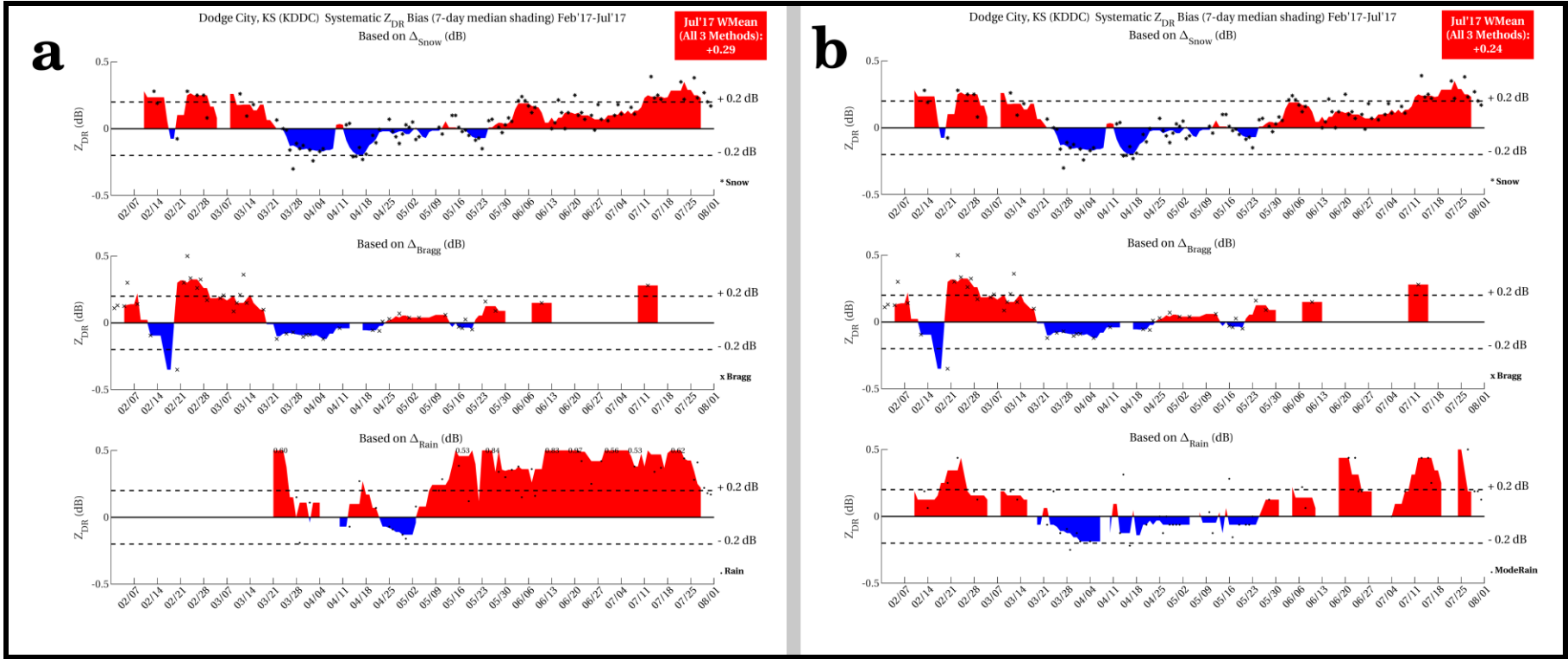FIGURE 11. Same as Figure 9 but for Minneapolis, MN (KMPX).

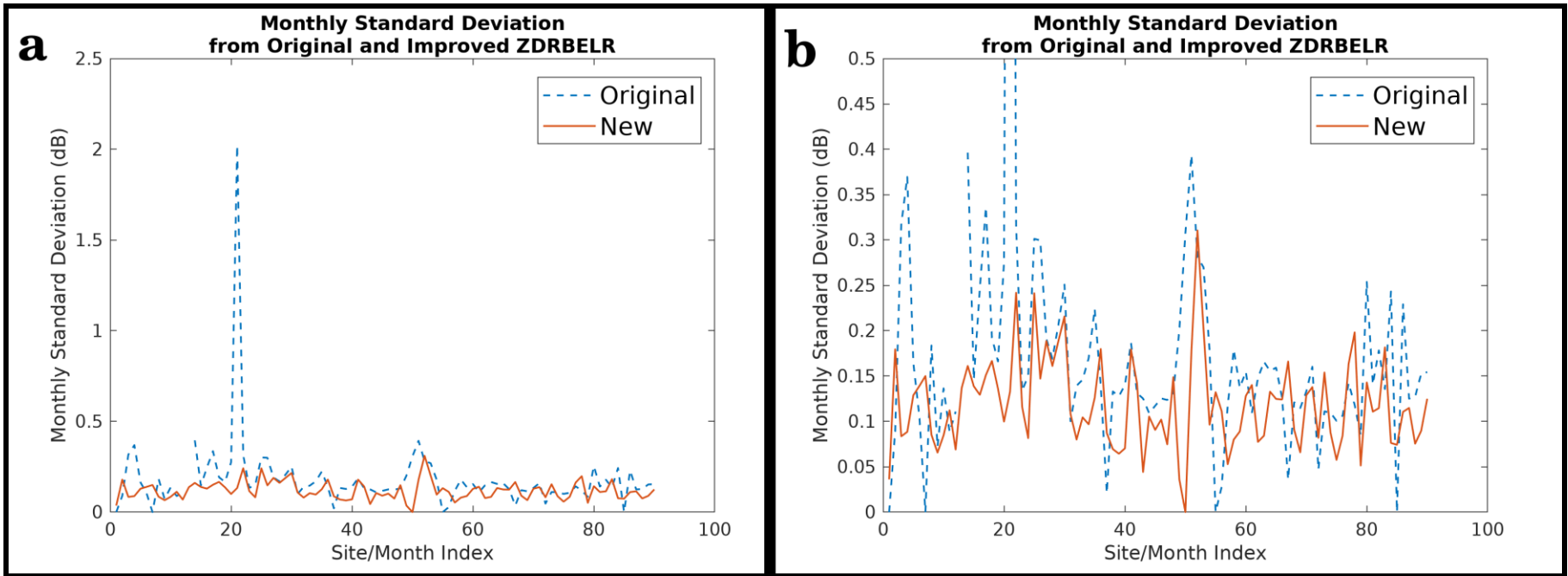FIGURE 12. Same as Figure 9 but for Dodge City, KS (KDDC).

FIGURE 13. Monthly Standard Deviations for each Site/Month combination used in the Verification data set with the original (dash blue) and New (Solid Orange) method of ZDRBELR. (a) Full scale view showing the singular large outlier near combination index 20. (b) Axes-limited view of the data in (a) for clarification of differences between the two methods.
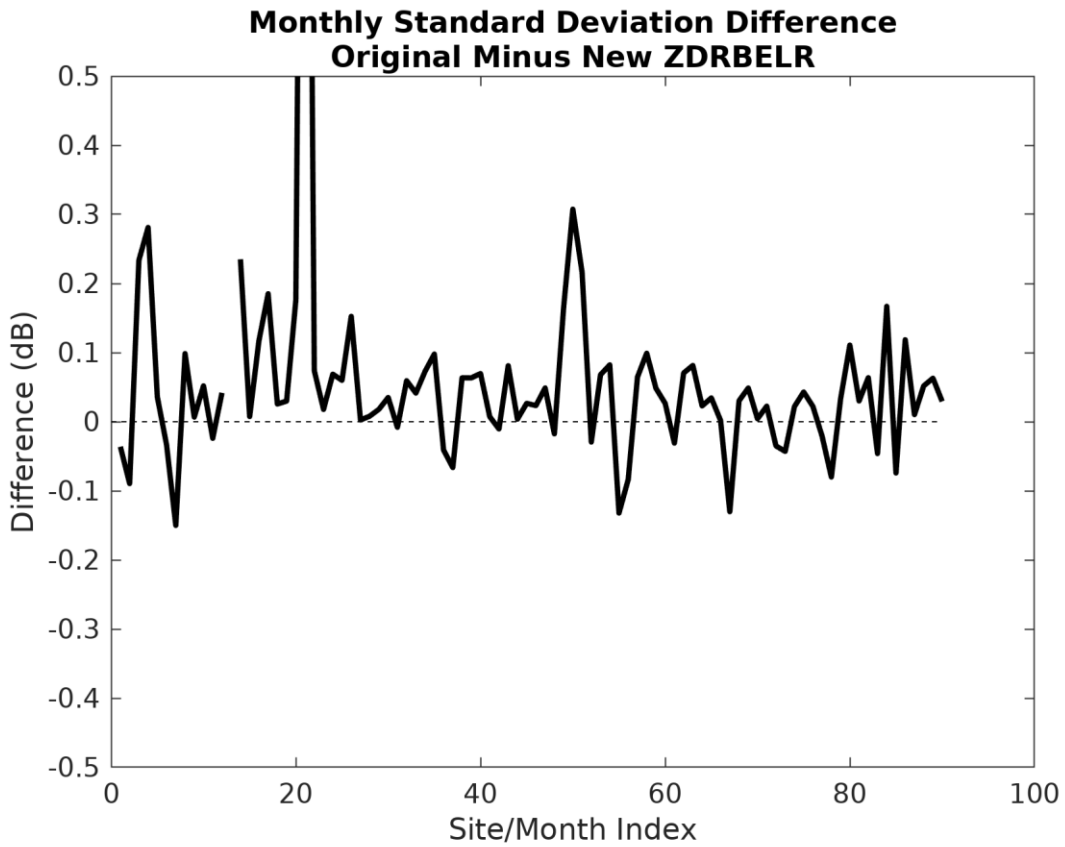
FIGURE 14. Differences of the results shown in Figure 13. The dashed line at 0 is meant as a visual marker to ease discernment of increased standard deviation with the Original or New ZDRBELR method.